Electrodiffusion Method of Near-Wall Flow Diagnostics in Microfluidic Systems

Jaroslav TIHON*, Vera PENKAVOVA, Petr STANOVSKY, Jiri VEJRAZKA

* Corresponding author: Tel.: ++420 220390250; Email: tihon@icpf.cas.cz
Institute of Chemical Process Fundamentals, Academy of Sciences of the Czech Republic, CZ

Abstract The electrodiffusion technique has been mostly used for the near-wall flow diagnostics on large scales. A novel technique for fabrication of plastic microfluidic systems with integrated metal microelectrodes (called technique of sacrificed substrate) enables us to produce microfluidic devices with precisely shaped sensors for wall shear stress measurements. Several micrometer thick gold sensors built-in a plastic substrate exhibit good mechanical resistance and smoothness. Proper functioning of prepared chips with microsensors has been first tested in various calibration experiments (polarization curve, sensor response to polarization set-up, steady flow calibration, temperature dependence of diffusivity). Our first results obtained for separating/reattaching flow behind a backward-facing step and for gas-liquid Taylor flow in microchannels then demonstrate its applicability for the detection of near-wall flow reversal, the delimitation of flow-recirculation zones, and the determination of wall shear stress response to moving bubbles. Other applications of these sensors in microfluidics (e.g. characterization of liquid films, capillary waves, bubbles or drops) can be also envisaged.

Keywords: Electrodiffusion Method, Wall Shear Stress, Microchannel Flow, Backward-Facing Step

1. Introduction

The electrodiffusion technique (see Selman and Tobias 1978, Hanratty and Campbell 1983), which has been until now used only for the near-wall flow diagnostics on larger scales, can be promising for both, scientific experiments and microdevice diagnostics. The electrodiffusion sensors prepared by the photolithography have been already applied to investigate the structure of near-wall turbulence in channel flows (see Deslouis et al. 2004) and their application in microfluidic systems has been just considered (see Illa et al. 2010, Mouheb et al. 2011, Abi-Samra et al. 2013). New microfabrication techniques enable us to produce microfluidic devices with precisely shaped microelectrodes. It offers a possibility to use such electrodiffusion sensors for near-wall flow investigations in various microfluidic systems (e.g. complex channels, micromixers, or multiphase microfluidic systems with bubbles and drops).

2. Electrodiffusion method

2.1 Principle of the method

The electrodiffusion sensor works as a small electrode, on which a fast electro-chemical reaction takes place, when a small polarization voltage is applied to it. The electric current passing through the electrode is the measured quantity. The current signal I provided by a simple strip probe is controlled by convective diffusion and depending on the wall shear rate γ according to the well-known Léveque formula

$$I = 0.807\, n F c_0 w l^{2/3} D^{2/3} \gamma^{1/3}, \qquad (1)$$

where n is the number of electrons involved in the electrochemical reaction, F is the Faraday constant, l is the length of the strip sensor in the mean flow direction, w is its width, c_0 is the bulk concentration of the active ions, and D is their diffusivity in the solution. The main advantage of this technique is that the wall probes provide information about the flow in the near wall region without any disturbances imposed on the studied velocity field.

If flow reversal occurs in the near-wall flow region and additional information on the flow direction is needed, a two-segment probe (see Son and Hanratty 1969) is usually applied. The instantaneous flow direction is determined by simple comparison of current signals obtained from the upstream (I_1) and downstream (I_2) probe segment. The rear segment (in respect to the actual flow direction) is located in a concentration shade of the front one and thus is giving the lower signal. Therefore, a possible near-wall flow reversal is detected from a sudden change of I_1/I_2(t) current ratio signal (from I_1(t) > I_2(t) to I_2(t) > I_1(t)). This criterion can be easily used to localize the stagnation points between steady recirculation-flow regions. Thorough discussion on the application of two-segment probes (especially analysis of their dynamic behavior) can be found in Tihon et al. 2003.

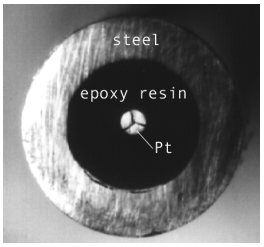

Fig.1. The three-segment probe (magnified front view).

The three-segment probe shown in Fig. 1 is able to evaluate not only the velocity but also the exact direction of near-wall flow. This circular probe is made from three platinum wires deformed by pulling together through a goldsmith-wiredrawing die (Sobolik et al. 1990). If the three-segment probe has identical segments, its total current I depends only on the absolute value of the wall shear rate vector γ and not on the probe configuration with respect to the flow direction. However, the probe configuration determines how the total current is divided between the individual current contributions I_s. Consequently, the ratio I_s/I is only a function of the flow direction angle Φ and can be expressed as a series

$$I_s/I = A_{s0} + \sum_{m=1}^{M} [A_{sm}\cos(m\Phi) + B_{sm}\sin(m\Phi)], \quad (2)$$

the so-called directional characteristics of the probe. As real probes have not geometrically identical segments, the calibration coefficients A_{sm} and B_{sm} have to be determined experimentally.

2.2 Sensor fabrication

Classical electrodiffusion probes (as that from Fig. 1) are fabricated from platinum or nickel foils or wires, which are glued into the wall of an experimental set-up. To produce precisely shaped microelectrode arrays, the application of photolithography is inevitable.

The deposition of planar microelectrodes on the microchip substrate is usually done in the form of thin metal films (gold, platinum, titan, nickel). The metallization is carried out by using galvanization, sputtering or vapor deposition techniques. The electrode pattern is transferred, via a photolithographic mask, into a thin film of photoresist material deposited on the substrate. A sequence of fabrication steps, including photoresist removal, electro-deposition, casting and etching, then complete the process of microelectrode fabrication.

An array of gold microelectrodes on a silicon wafer prepared for a near-wall turbulence study is shown in Fig. 2. There are two masks levels applied: the first one corresponds to the overall design including both the active areas and the paths for the current to the measuring device. The second one is aimed at coating this latter part and avoiding it to be in contact with the solution. The thickness of deposited layers (active gold and protective silicon nitride) is 0.3 μm. Therefore, the surface of microchip can be considered as relatively smooth.

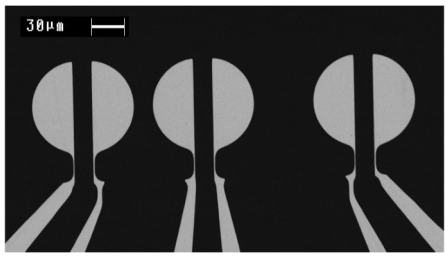

Fig. 2. Double semi-circular microsensors prepared by the photolithography (Deslouis et al. 2004).

A novel technique for fabrication of plastic microfluidic systems with integrated metal

microelectrodes (called technique of sacrificed substrate) has been developed in the Laboratory of Microtechnology at the Institute of Chemical Technology in Prague (see Schrott et al. 2009). This fabrication technique includes: (i) optical photolitho-graphy in the photoresist previously coated on a metal substrate, (ii) electroplating of gold sensors, (iii) photoresist stripping, (iv) embedding of the gold sensors in the UV curable resin Acrifix 192®, (v) UV curing of the resin, and (vi) removal of the metal substrate by etching. Relatively high thickness (several micro-meters) of the gold sensor built-in in PMMA resin provides both, a good mechanical resistance and surface smoothness. The chip with microsensors fabricated by this technique has been used in this work.

2.3 Calibration procedure

The Léveque formula (Eq.1) relates the instantaneous values of wall shear rate and limiting diffusion current only if measured flow fluctuations are slow enough (quasi-steady). For proper use of sensors under unsteady flow conditions, it is necessary to consider their dynamic response. The approximate model suggested for description of the probe dynamic behaviour (see Sobolik et al. 1987, Tihon et al. 1995) is represented by a simple formula

$$\gamma = k_s^{-3}\left(I^3 + 2k_t^2 \frac{dI}{dt} \right). \tag{3}$$

This semi-empirical differential equation contains two constants, easily accessible from calibration experiments.

If the exact shape of a probe and the diffusivity and concentration of ions involved in the electrode reaction are known, they can be also calculated from the theoretical relationships. Considering a single strip probe, the first constant k_s is obtained from the steady state solution (Eq.1), which provides

$$k_s = 0.807 z F c_0 w l^{2/3} D^{2/3}. \tag{4}$$

The second constant k_t can be determined from the known solution of unsteady diffusion at the beginning of transient process after the polarization switch-on

$$I = k_t\, t^{-1/2} \tag{5}$$

with

$$k_t = z F c_0 w l \sqrt{D/\pi}\,. \tag{6}$$

To estimate the dynamic behaviour of a single probe at given flow conditions (characterised by the mean value of γ), the characteristic time parameter t_0 can be introduced as

$$t_0 = (k_t/\bar{I})^2 = (k_t/k_s)^2\, \gamma^{-2/3}. \tag{7}$$

This parameter is determined as the time coordinate of the intersection of both the asymptotes (Eq.1 and Eq.5) of the transient current response after the probe polarization switch-on. The dependence of this characteristic time on actual flow conditions represented by the mean value of wall shear rate is an important consequence of nonlinear dynamic behaviour of the electrodiffusion probes.

2. Experiments in microchannels

2.1 Sensors and electrolyte

A measuring chip with sensors fabricated by the method of a sacrificed substrate consists of an array of gold strips embedded into a Plexiglas plate (see Fig. 3). Twenty sensing cathodes (160 μm strips) separated by 40 μm insulating gaps are located between two large anodes (10 mm strips). The design of the chip enables us to use cathodes as individual (strip) or double (two-strip) sensors. The plate with microelectrodes serves as a top cover (roof wall) of several microchannel devices.

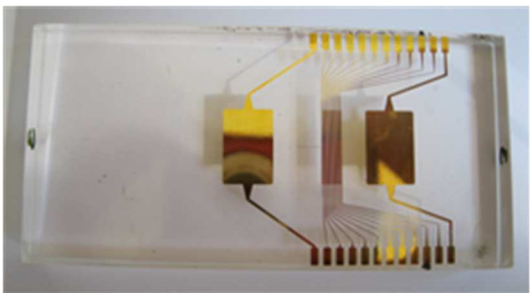

Fig. 3. Measuring chip with the gold strip sensors (20 cathodes located between 2 large anodes).

Water with equimolar 0.002 M potassium ferrocyanide and ferricyanide is used as a

suitable electrochemical system and 0.2 M potassium sulfate as a supporting electrolyte. The resulting solution has a density of ρ =1024 kg/m^3 and a kinematic viscosity of ν = 1.06 mm^2/s at a reference temperature of 22ºC. The polarization voltage of -0.6 V applied between sensing electrodes and counter-electrodes assures that ferricyanide ions reduce on the electrode surface and the resulting current is limited by the convective diffusion. An in-house electrodiffusion device is used to apply the polarization voltage, to convert currents through the individual sensors into voltage signals, and to amplify them. The device is controlled by a computer, which also records the measured signals.

2.2 Experimental apparatus

Two microchannels with rectangular cross-sections (200 and 800 μm in height and 10 mm in width) are applied for the calibration of sensors. Their length of 80 mm is sufficient to achieve developed flow conditions at the measuring locations. The active surface of sensors is delimited by a sealing located between the microchannel and measuring chip and thus forming side walls of microchannels. Both these parts are fixed into a clamp table, which enables to shift the chip with sensors in respect to the channel inlet (see Fig. 4). Two gear pumps Heidolph and Micropump are used to supply the electrolyte into the microchannel, covering the range Q_L from 7 to 500 ml/min.

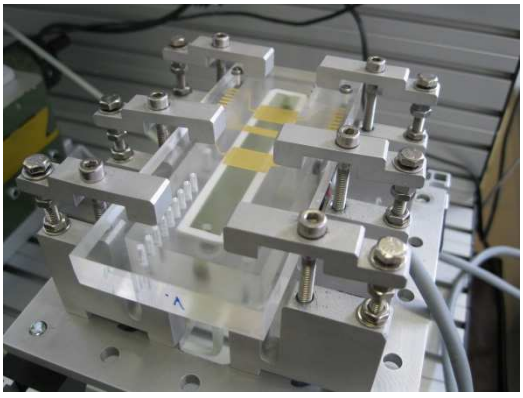

Fig. 4. Experimental apparatus

A stainless steel foil (thickness of 400 μm) is used to form a backward-facing step (with an expansion ratio *ER*=2) inside the deeper microchannel. A capillary (20 μm i.d.) is placed into inlet tubing to inject air into the microchannel and thus produce gas-liquid Taylor flow. The bubble growth is controlled by adjusting the pressure and opening times of two (inlet and vent) electromagnetic valves

3. Results and discussion

3.1 Sensor testing and calibration

Proper functioning of prepared sensors has been first tested by the measurement of polarization curves (see Fig. 5). As currents measured at moderate polarization voltages (around U~-0.5V) are limited by diffusion of the active ions towards the sensor surface, the observed polarization curves are characterized by distinct plateaus. The current at plateaus is sensitive to actual flow conditions (i.e. wall shear rate magnitudes) in the microchannel. The polarization voltage of -0.6 V has been chosen for following calibrations and measurements.

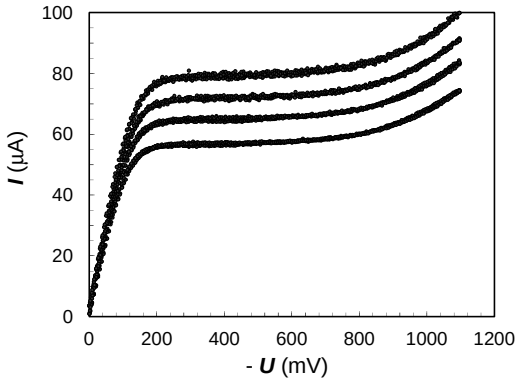

Fig. 5. Limiting diffusion currents measured at different flow rates (for γ=3120, 4690, 6250, and 7810 s^{-1}).

Practically same polarization curves have been obtained for all tested sensors. The individual currents from sensors for the same flow rates have been differentiated less than 0.5%. The results of sensor calibration carried out under steady laminar flow conditions are shown in Fig. 6. The measured currents follow very well a cubic root dependence on the wall shear rate prescribed by Eq.1. The calibration constant k_s=3.52 μA.s$^{1/3}$ is determined from data fit (see dash line). As the electrolyte concentration and sensor dimensions are known, Eq.4 provides for the diffusion

coefficient of ferricyanide ions an estimate of $D = 6.7\ 10^{-10}$ m^2/s. This value (measured at temperature of $T = 22$ °C) is in a good agreement with the previous experimental findings (see Eroglu et al. 2011).

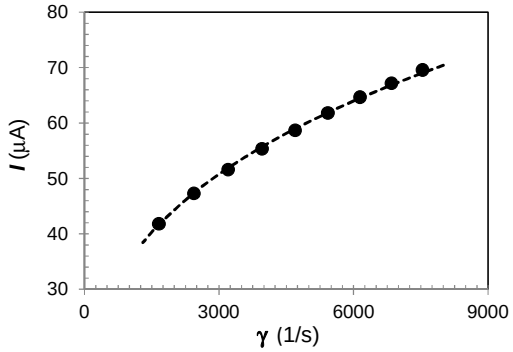

Fig. 6. Sensor calibration at the steady flow conditions (dash line stands for data fit: I=3.52 $\gamma^{1/3}$).

The transient current response to a set-up of polarization voltage, obtained for the sensor in stagnant electrolyte, is presented in Fig. 7.

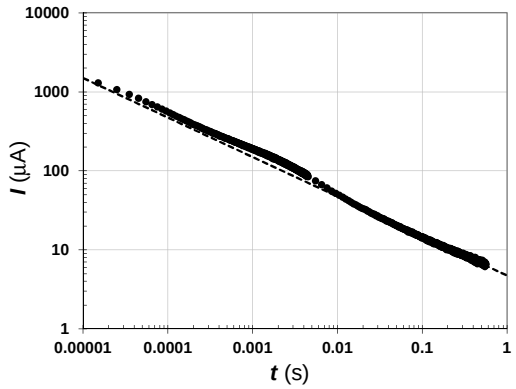

Fig. 7. Transient current response to the set-up of polarization voltage measured in stagnant electrolyte (dash line stands for low current data fit: I=4.7 $t^{-1/2}$).

The measured data are controlled by unsteady diffusion at the beginning of transient process and can be fitted well by the Cottrell asymptote (Eq.5). then provides The diffusion coefficient of $D = 7.3\ 10^{-10}$ m^2/s corresponds according to Eq.6 to the dynamic calibration constant k_t=4.7 μA.s$^{1/2}$ obtained from this dynamic calibration. As this value agrees satisfactorily with that obtained from the steady calibration, the proper functioning of sensors is verified.

The sensitivity of measurements to the temperature changes has been also tested. The electrolyte reservoir has been placed into a thermostat and its temperature precisely controlled. The temperature dependence of diffusivity determined from the results of steady flow calibrations done at different temperatures is shown in Fig. 8.

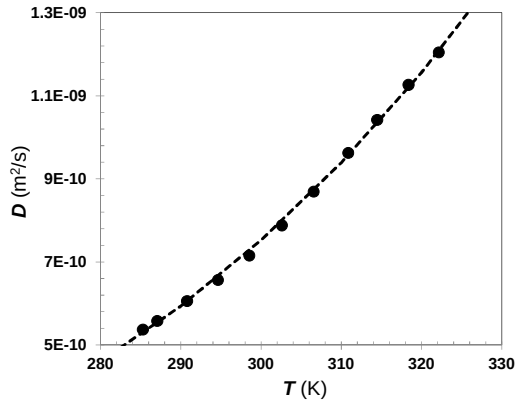

Fig. 8. Temperature dependence of the diffusivity (dash line stands for exponential fit: $D = 7.26.10^{-7}\ e^{-(2061/T)}$).

As expected the diffusion coefficient is strongly dependent on temperature and the measured data can be fitted by an exponential relationship (similar to Arrhenius equation $D=A_0\ e^{(E/RT)}$, where E and R are the activation energy barrier and universal gas constant, respectively). The viscosity and diffusivity of liquids can be related to each other in the form of traditional Stokes-Einstein parameter $D\mu/T$=const. This parameter is found to be practically constant also for our electrolyte. The value of $D\mu/T = 2.2\ 10^{-15}$ N.K^{-1} calculated from measured diffusivity and viscosity data falls well into the range $2.0 \div 2.8\ 10^{-15}$ N.K^{-1} determined for ferricyanide ions and different supporting electrolytes in the previous measurements (see Arvia et al. 1967).

The errors of wall shear rate measurements connected with current sensing, calibration procedures, possible temperature fluctuations are estimated not exceed the level of 10%.

3.2 Backward-facing step flow

To measure the wall shear rate profile behind a backward-facing step (channel height H=800 μm, step height h=400 μm), sensors are used as double (two-strip) sensors and the measuring chip is subsequently fixed at four positions (the first sensor at x_0=0, 4, 8, 12 mm)

to cover the measuring range x/h from 0 to 40. At low flow rates (for $\mathrm{Re}=2UH/\nu < 600$), the backward-facing step flow is found to be steady without any significant fluctuations. The position of reattachment is fixed and the wall shear rate should be equal to zero there. The typical wall shear rate profiles measured under still steady laminar flow conditions (at Re = 625) are presented in Fig. 9. As the flow in a flat channel is predominantly two-dimensional, the obtained experimental data are in good agreement with the results of our previous 2D numerical simulations (see Tihon et al. 2010). The axial profile obtained at the bottom wall exhibits a strong negative peak corresponding to flow reversal inside a primary recirculation zone (for x/h from 0 to 9.75), which is followed by a region of slow recovery to the channel flow (for x/h from 9.75 to 40). The exact position of reattachment point is determined from measured I_2/I_1 (x/h) profile (I_2/I_1=1 for $x=x_r$). The wall shear rate profile measured at the roof wall shows that the near-wall flow is very close to separation there.

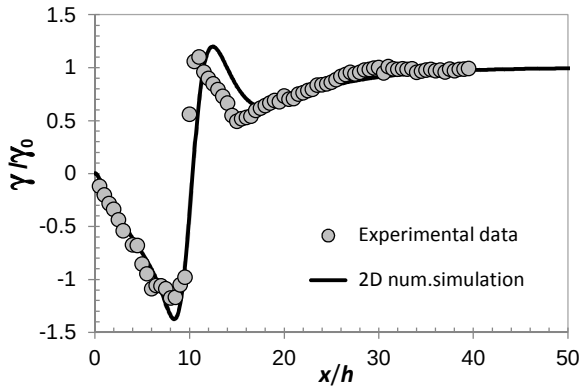

Fig. 9. Wall shear rate profile behind the step at Re=625 (γ_0=2930 $s^{-1}$for the fully developed channel flow).

As soon as the flow separation at the roof leads to the inception of a recirculation eddy, the flow configuration with two flow-recirculation regions becomes unsteady and flow fluctuations originated from the separated shear layer are progressively amplified in the recirculation regions. Unsteady character of near-wall flow inside the reattachment region is shown in Fig. 10.

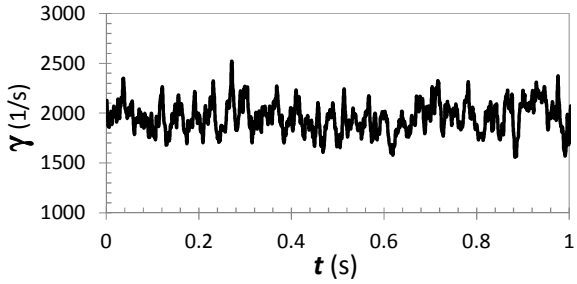

Fig. 10. Time trace of wall shear rate measured behind the reattachment at x/h=13.5 and Re=1105.

As the wall shear rate magnitude ($\gamma \sim U/H$) in microchannels is much higher than in common channels, also the frequency range of observed flow fluctuations is significantly higher. Therefore, to find frequency scaling of fluctuations from the spectral analysis, the dynamic behavior of sensors has to be considered. To capture correctly possible small and high-frequency fluctuations induced by a micro backward-facing step, smaller sensor sizes are also needed. This experiment is now in preparation.

3.3 Gas-liquid Taylor flow in microchannel

Gas-liquid Taylor flow experiments have been carried out in the microchannel with H=800 μm, which has been oriented either horizontally or vertically. Typical electro-diffusion data measured during the rise of a single large bubble in the vertical micro-channel are shown in Fig. 11. In this case, a flat bubble (V_B=60 μl) with a typical "bullet-like" outline was rising in co-flowing liquid (U_L=0.0156 m/s). The current signals recorded from two sensors (1st and 20th sensor from the array) are presented in Fig. 11a and the corresponding time series of wall shear rate is shown in Fig. 11b. The bubble rise velocity (U_B = 0.0418 m/s) is calculated from the time shift Δt=91 ms between two current signals measured by the sensors separated by the distance Δx=3.8 mm. Even though the channel height is less than 1 mm, buoyancy still play an important role (bubble velocity measured in stagnant liquid is U_{B0} = 0.03 m/s). The trace of wall shear rate corresponding to the near-wall flow around the rising bubble exhibits two peaks (the first at bubble front, the second at

bubble back), which are separated by the region of small wall shear rates (almost stagnant liquid film located between the flat side of bubble and the wide wall of micro-channel).

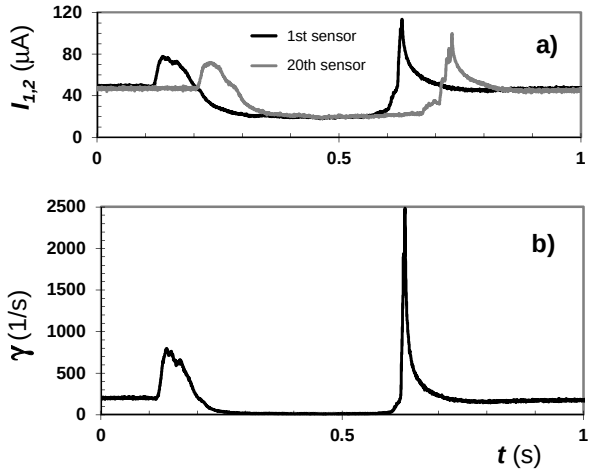

Fig. 11. Response of electrodiffusion signals to a rising bubble (H=0.8 mm, W=10 mm, U_B=0.042 m/s V_B=60 μl,): (a) currents from two sensors, (b) wall shear rate calculated from the primary current signal.

This wall shear rate profile differentiates significantly from those measured in large channels, where the strong reverse flow in the liquid film under the bubble and highly unsteady flow behind the bubble are observed. It is documented in Fig. 12, where the wall shear rate data measured in a rectangular channel with the cross-section 4 x 50 mm are shown (see Tihon et al. 2013).

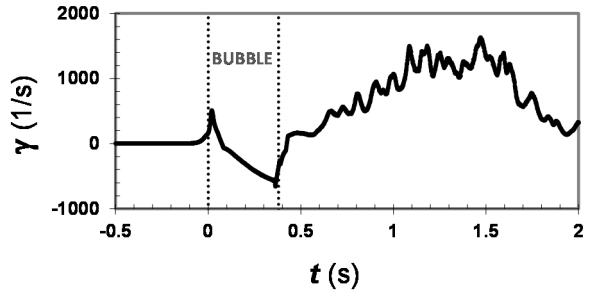

Fig. 12. Wall shear rate induced by a rising bubble in stagnant water in the vertical rectangular channel (H=4 mm, W=50 mm, V_B=8 ml, U_B=0.156 m/s).

The velocity of bubble translation U_B in liquid co-flowing with the mean velocity U_L can be expressed as a sum of two components: the bubble velocity in stagnant liquid U_{Bo} and a component proportional to the mean liquid velocity

$$U_B = U_{Bo} + C_0 U_L \quad . \tag{8}$$

As seen in Fig. 13, this linear relationship holds also in microchannels. However, the distribution coefficient C_0 is significantly smaller than in large channels, where its value is controlled by the maximum liquid velocity at the channel center-line (thus for the laminar flow in a flat channel C_0~1.5). Magnitude of C_0 is found to be sensitive also to the channel inclination. In the horizontal microchannel the bubble velocity is only about 5% higher than the mean velocity of co-flowing liquid.

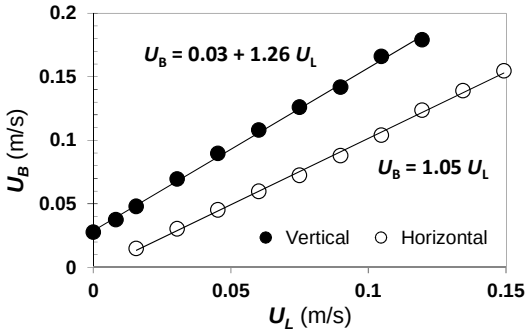

Fig. 13. Velocities of large bubbles translating in co-flowing liquid measured for the vertical and horizontal orientation of the microchannel.

4. Conclusions

The chip with electrodiffusion sensors fabricated by the method of a sacrificed substrate proved to be a reliable platform for the flow diagnostics in microfluidic devices. Our first results obtained for separating and reattaching flow behind a backward-facing step and for gas-liquid Taylor flow in microchannels demonstrate its applicability for the detection of near-wall flow reversal, the delimitation of flow-recirculation zones, and the determination of wall shear stress response to moving bubbles. Other applications of these sensors in microfluidics (e.g. characterization of liquid films, capillary waves, bubbles or drops) are also envisaged.

Acknowledgement

The support by Czech Science Foundation GACR through the contract P101/12/0585 is gratefully acknowledged.

References

Abi-Samra, K., Kim, T.H., Park, D.K., Kim, N., Kim, J., Kim, H., Cho, Y.K., Madou, M., 2013. Electro-chemical velocimetry on centrifugal microfluidic platforms. *Lab on a Chip*, 13, 3253-3260.

Arvia, A.J., Marchian S.L., Podesta, J.J., 1967. Diffusion of Ferrocyanide and Ferri-Cyanide Ions in Aqueous Solutions of Potassium Hydroxide. *Electrochimica Acta*, 12, 259-266.

Deslouis, C., Tribollet, B., Tihon, J., 2004. Near-wall turbulence in drag reducing flows investigated by the photolithography-electrochemical probes. *J. Non-Newt. Fluid Mech.*, 123, 141-150.

Eroglu, E., Yapici, S., Sara, O.N., 2011. Some Transport Properties of Potassium Ferri/Ferro-Cyanide Solutions in a Wide Range of Schmidt Numbers. *J.Chem.Eng. Data*, 56, 3312-3317.

Hanratty, T.J., Campbell, J.A., 1983. *Measurement of wall shear stress*, in 'Fluid mechanics measurements' (edited by J.R. Goldstein, Washington, Hemisphere) pp. 559-615.¨

Illa, X., Ordeig, O., Snakenborg, D., Romano-Rodriguez, A., Compton, R.G., Kutter, J.P., 2010. A cyclo olefin polymer microfluidic chip with integrated gold microelectrodes for aqueous and non-aqueous electrochemistry. *Lab on a Chip*, 10, 1254-1261.

Mouheb, N. A., Montillet, A., Solliec, C., Havlica, J., Legentilhomme, P., Comiti, J., Tihon, J., 2011. Flow characterization in T-shaped and cross-shaped micromixers. *Microfluid. Nanofluid.*, 10, 1185-1197.

Schrott, W., Svoboda, M., Slouka, Z., Snita, D., 2009. Metal electrodes in plastic microfluidic systems. *Microelectronic Engineering*, 86, 1340-1342.

Selman, J.R., Tobias, Ch.V., 1978. *Mass-transfer measurements by the limiting-current technique*, in: Advances in Chem.Engineering (edited by T.B.Drew, G.R.Cokelet, J.W.Hoopes, T.Vermeulen, Acad.Press, NY) pp. 211-318.¨

Sobolik, V., Wein, O., Cermak, J., 1987. Simultaneous Measurement of Film Thickness and Wall Shear-Stress in Wavy Flow of Non-Newtonian Liquids. *Collect. Czech. Chem. Com*, 52, 913-928.

Sobolik, V., Wein, O., Gil, O., Tribollet, B., 1990. 3-Segment Electrodiffusion Probes for Measuring Velocity-Fields Close to a Wall. *Exp. Fluids*, 9, 43-48.

Son, J.S., Hanratty, T.J., 1969. Velocity Gradients at Wall for Flow around a Cylinder at Reynolds Numbers from 5x103 to 105. *J. Fluid Mech.* 35, 353-368.

Tihon, J., Legrand, J., Aouabed, H., Legentilhomme, P., 1995. Dynamics of Electrodiffusion Probes in Developing Annular Flows. *Exp. Fluids*, 20, 131-134.

Tihon, J., Tovchigrechko, V., Sobolík, V., Wein, O., 2003. Electrodiffusion detection of the near-wall flow reversal in liquid films at the regime of solitary waves. *J. Appl. Electrochem.* 33, 577-587.

Tihon, J., Penkavova, V., Pantzali, M., 2010. The effect of inlet pulsations on the backward-facing step flow, *Eur.J.Mech.,B/Fluids* 29, 224-235.

Tihon, J., Penkavova, V., Vejrazka, J., 2013. Wall Shear Stress Induced by Taylor Bubbles in Inclined Flow Channels, *EPJ Web of Conferences* 45, 01089 (2013)